Taylor & Francis
Taylor & Francis Group

Vehicle System Dynamics
International Journal of Vehicle Mechanics and Mobility

ISSN: 0042-3114 (Print) 1744-5159 (Online) Journal homepage: http://www.tandfonline.com/loi/nvsd20

Improvements for the stability of heavy-haul couplers with arc surface contact

Guosong Wu, Huang Wang & Yuan Yao

To cite this article: Guosong Wu, Huang Wang & Yuan Yao (2018) Improvements for the stability of heavy-haul couplers with arc surface contact, Vehicle System Dynamics, 56:3, 428-442, DOI: 10.1080/00423114.2017.1381982

To link to this article: https://doi.org/10.1080/00423114.2017.1381982

Published online: 04 Oct 2017.

VEHICLE SYSTEM DYNAMICS, 2018
VOL. 56, NO. 3, 428–442
https://doi.org/10.1080/00423114.2017.1381982

Improvements for the stability of heavy-haul couplers with arc surface contact

Guosong Wu, Huang Wang and Yuan Yao

State Key Laboratory of Traction Power, Southwest Jiaotong University, Chengdu, People's Republic of China

ABSTRACT
To investigate the stability mechanism of heavy-haul couplers with arc surface contact, the geometry and force analysis were conducted according to the friction circle theory. To improve the stability of the coupler, four improvements were proposed, which are increasing the secondary lateral stiffness of locomotives, adding a restoring bumpstop at the end of the coupler, increasing the arc surfaces radii and changing the clearance and stiffness of secondary lateral stopping block. A multi-body dynamics model with four heavy-haul locomotives and three detailed couplers were established to simulate the emergency braking. In addition, the coupler yaw instability was tested to investigate the effects of relevant parameters on the coupler stability. The results show that increasing the secondary lateral stiffness of locomotives, adding a bumpstop with a smaller bumpstop gap, increasing the arc surfaces radii, increasing the stiffness and decreasing the clearance of secondary lateral stopping block are conducive to improving the stability of the coupler with arc surface contact.

ARTICLE HISTORY
Received 3 March 2017
Revised 10 August 2017
Accepted 10 September 2017

KEYWORDS
Heavy-haul couplers; coupler stability; improvements; locomotive; derailment

1. Introduction

The large longitudinal compression forces make the coupler yaw unstable during the emergency braking. Coupler yaw instability causes the larger lateral forces and even leads to derailment. The derailment caused by coupler yaw occurs occasionally when the train is in emergency braking [1–5]. Such derailments have drawn the attention of design, production and application departments.

Cole performed many studies on the heavy-haul trains and has presented many papers concerning the problems of heavy-haul trains, such as longitudinal train dynamics, the modelling of the wagon connection model, comfort and train management and driving practices [6–8]. A comprehensive nonlinear model was developed in [9] to study train derailment and hunting in severe braking conditions to minimise the tendency of train derailment. For the braking safety problem of the heavy-haul trains, the Association of American Railroads [10] has introduced provisions in certain aspects, such as coupler design standard, air braking and train manoeuvring.

CONTACT Yuan Yao yyuan8848@163.com

The couplers of heavy-haul locomotives widely used in China can be divided into two types according to their structure. For the first type, there is an arc contact surface at the end of the coupler. The coupler longitudinal forces are transferred by arc contact surface when compressed. Xu et al. [11] studied the coupler rotation behaviour, and concluded that decrease the maximum coupler free angle can improve the locomotives' operational performance, and recommended to limit it to 4 degrees. Shi et al. [12] investigated the effect of arc surfaces friction coefficient on coupler stability by simulation and field tests. The results show that increasing the friction coefficient can improve the coupler stability. Yao et al. [13] analysed the stability mechanism of the coupler with friction circle theory and underlined the importance of the arc contact surfaces friction coefficient and the secondary lateral stiffness of locomotives. Wu et al. [14] used rotate joint to simulate the yoke key of the coupler and proposed that the yaw moment caused by the coupler yaw angle will be balanced by the friction torque supplied by the arc contact surfaces. For the second type, there is an elastic stopper which can limit the coupler yaw angle to ensure the stability of the coupler. Yao et al. [15] analysed the structure and mechanical characteristics of the coupler and proposed the matching principle with the locomotive secondary suspension parameters for a smaller wheelset lateral force during braking. Ma and Luo [16,17] have studied the effects of the coupler and buffer systems on the dynamic performance of heavy-haul locomotives. Yao et al. [18] proposed an innovative heavy-haul coupler that integrates the merits of both types of couplers and conducted the dynamics simulation to verify the feasibility.

Current studies assumed the increasing of the arc surfaces friction coefficient to be ideal and suggested that the friction coefficient should be 0.3 or higher. However, the limitation of increasing friction coefficient should not be ignored for engineering guidance. Considering the limited time and money, and combining the practical and theoretical considerations, four improvements were proposed in this paper to improve the stability of the coupler with arc surface contact according to the structure characteristics and stability mechanism of the coupler.

2. The structure characteristics and stability mechanism of the coupler

2.1. The coupler structure

The detailed structure of diesel-electric locomotive coupler used in China has been introduced in [18], as shown in Figure 1. It is mainly composed of a coupler yoke, rubber buffer, follower, yoke key and coupler. The coupler and coupler yoke are connected by yoke key, and both the coupler end and the follower have arc contact surfaces. When the coupler pulled, it pulls the yoke key and moves the coupler yoke, leading to compressing the rubber buffer, thus providing the longitudinal traction stiffness and damping. When the coupler is compressed, the yoke key cannot transfer the longitudinal compressive force, and it is transferred by the arc surface contact and thus compressing the rubber buffer. The arc radii of the follower and the end of the coupler are 150 and 130 mm, respectively. The different arc radii lead to the rolling contact motion between the two arc surfaces, rather than pure sliding, which is the key of this kind of coupler.

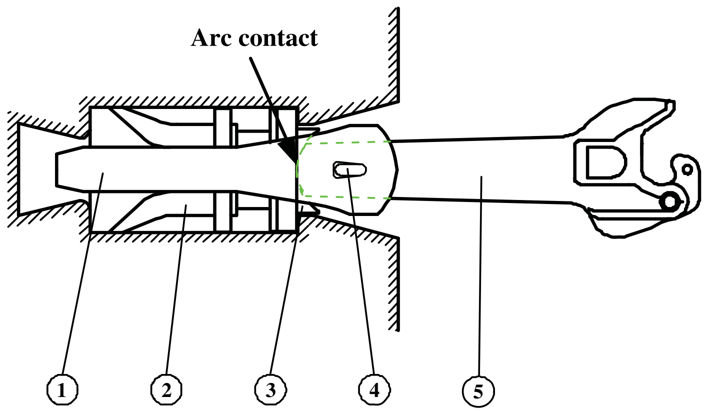

1. Coupler yoke, 2.Rubber buffer, 3.Follower, 4.Yoke key, 5.Coupler

Figure 1. The structure of diesel-electric locomotive coupler with arc surface contact.

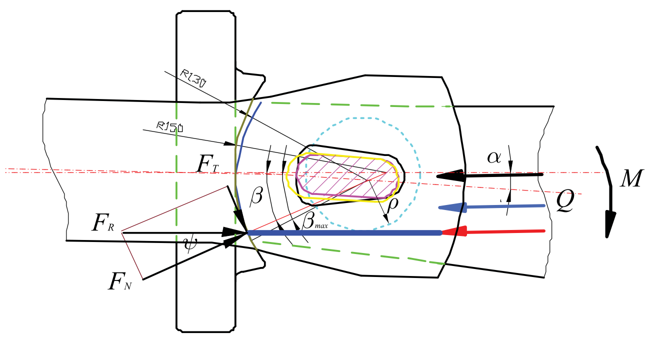

Figure 2. The contact analysis of the end arc surfaces.

2.2. The contact analysis of arc surfaces

According to the contact analysis of arc surfaces in [18], the contact between the follower and the coupler is line contact because of the two different radii. The contact analysis of the end arc surfaces is shown in Figure 2. When the coupler rotates and the yaw angle is α, the contact point moves along the arc because of the tangential friction force. The angle between the contact point and the centre line of the follower is β, which is called the contact angle. Assuming that the friction of the contact surfaces is not saturated, the two arc contact surfaces are pure rolling. The relationship of α and β is as follows:

$$\beta = \frac{r}{R-r}\alpha. \tag{1}$$

According to the contact analysis of arc surfaces under braking conditions in [18], the coupler is acted upon by the longitudinal compression force, Q, and the yaw moment, M, when the coupler has a certain yaw angle during the braking process. The M can be equivalent to translating Q in the lateral direction for a distance of L, where $L = M/Q$. The moved force line is the actual force transmission line and passes through contact point. According to the friction circle theory, a friction circle with the radius of ρ is drawn in the centre of the arc surface at the end of the coupler. The relationship of the ρ and the friction coefficient of two arc contact surfaces is as follows:

$$\rho = r\sin(\tan^{-1}\mu). \quad (2)$$

When the L is smaller than ρ, the friction is not saturated and the contact between two arc surfaces is pure rolling. When the L equals to ρ, the contact is in the critical state and the force line is tangent to the friction circle. When the L is larger than ρ, the two arc contact surfaces slide and the contact point is located at the intersection of the force line and the arc surface. The angle α and β increase with the increase of the relative lateral displacement of the two car bodies at the beginning of the rolling contact process. When the angle α increases to a certain value, the arc friction is saturated and the two contact surfaces begin to slide. At this point, the angle β decreases as the α increases. The coupler experiences the tangent friction and the normal support force at the contact point. The force line is parallel with track at a small coupler yaw angle, where the arc friction is not saturated and there is not the coupler lateral force.

2.3. The stability mechanism of the coupler

The structure is symmetric when the two diesel-electric locomotives are connected. The force transmission line is located on the inner common tangent line of two friction circles at the two ends of the couplers in the critical roll-slip state, where the relative lateral displacement, Y_{b}, between the two car bodies connected by couplers are defined as the car body critical lateral displacement, Y_{bc}, and the corresponding coupler yaw angle is defined as the coupler critical yaw angle, α_{c}. The Y_{bc} and α_{c} are dependent on the arc contact surface friction coefficient μ. When the coupler yaw angle α is smaller than α_{c}, the direction of force line which is the connection line between the two arc contact points is consistent with the resultant force at the contact point.

The coupler mainly experiences longitudinal compressive force in the process of braking. The direction of force transmission line is parallel with the track for the coupler at a small yaw angle, where there is not coupler lateral force, as the state 1 in Figure 3. When the arc contact surfaces slide, the direction of resultant force at the contact point deflects the track and the coupler lateral force occurs, where the yaw angle of force transmission line is smaller than the actual yaw angle of the coupler, as the state 2 in Figure 3. When the friction coefficient of arc surface is large enough, the direction of resultant force at the contact point is along the direction of the force transmission line, and the arc contact surfaces will not slide. The force transmission line deviates from the direction of the track, which produces the coupler lateral force. The coupler lateral force causes the horizontal movement of car body and will be balanced by the locomotive secondary suspension. The coupler lateral force is transferred to the bogie, which will result in the increasing of wheelset lateral force. The coupler yaw angle becomes unstable and the locomotive will derail on condition that the coupler lateral force and the wheelset lateral forces cannot be balanced by the locomotive secondary suspension.

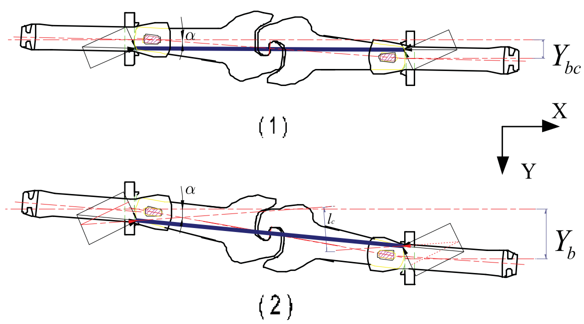

Figure 3. The two states of force transmission line.

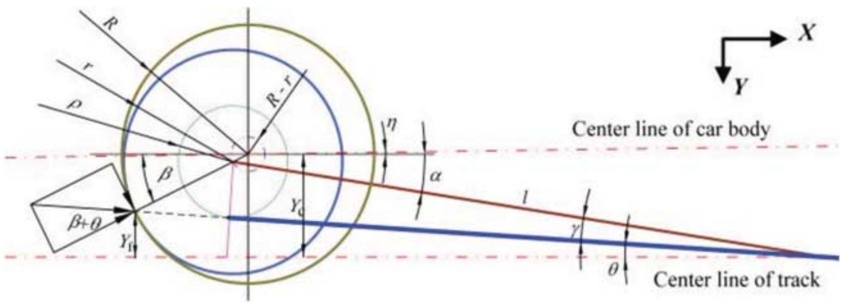

Figure 4. The geometric analysis of the coupler and the force line.

2.4. The geometric analysis of the coupler and the force line

The geometric relationships of the coupler and the force line are shown in Figure 4. Ignoring the car body yaw angle η, the geometric relationships between the angle of the force line to the track centreline θ and the angle of the force line to the coupler centreline γ are as follows:

$$\gamma = \sin^{-1}\left(\frac{\rho}{l}\right), \tag{3}$$

$$\beta + \theta = \tan^{-1}\mu, \tag{4}$$

$$\alpha = \gamma + \theta, \tag{5}$$

where l is half of the coupler length, and it is 712 mm for these studies.

When the matching of the two radii is optimal, the car body critical lateral displacement Y_{bc} is

$$Y_{\mathrm{bc}} = R\sin(\tan^{-1}\mu). \tag{6}$$

When $Y_{\mathrm{b}} \le Y_{\mathrm{bc}}$, the force line moves along the track direction, as states (1) and (2) in Figure 5.

When $Y_{\mathrm{b}} > Y_{\mathrm{bc}}$, the force line deflects the track direction as state (3) in Figure 5. There is a lateral force that appears between the two car bodies caused by the coupler.

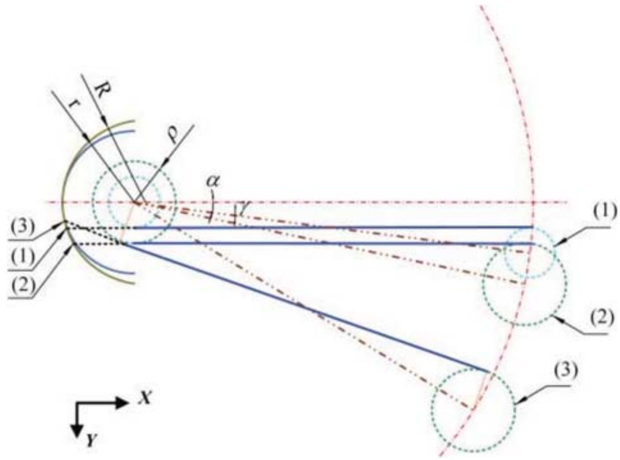

Figure 5. The three typical states of the force line.

In fact, the locomotive derailment occurs due to the excessive wheel–rail lateral forces when the coupler is yaw unstable. According to the biggest wheelset lateral force in BS EN 14363, the maximum permissible yaw angle of the force line can be calculated

$$\theta_{\max} \leq \tan^{-1}\left(\frac{L_b}{L_c F_{xc}}\left(10+\frac{2Q_0}{3}\right)\right), \tag{7}$$

where $L_b$and L_c are the longitudinal distance of the bogie centre and the fixing seats at both ends of car body separately. F_{xc} is the biggest coupler longitudinal force (kN). $2Q_0$ is the axle load of the locomotive (kN). According to the Formula (2)–(5), the maximum permissible yaw angle of the coupler is

$$\alpha_{\max} = \theta_{\max} + \sin^{-1}\left(\frac{r}{l}\sin(\tan^{-1}\mu)\right). \tag{8}$$

3. Improvements for the stability of the coupler

Based on the structure characteristics and the stability mechanism of the coupler, four schemes are proposed to improve the coupler yaw stability. For the first scheme, increasing the secondary lateral stiffness of locomotives is chosen as an effective way to improve the stability of the coupler. For the second scheme, we can add a restoring bumpstop at the end of the coupler to limit the coupler yaw angle. For the third scheme, increasing the arc radii at the end of the coupler can be an efficacious method according to the stability mechanism of the coupler. For the fourth scheme, the clearance and stiffness of secondary lateral stopping block are changed for the better stability of the coupler.

3.1. Increasing the secondary lateral stiffness of locomotives

According to the stability mechanism of the coupler, the coupler lateral forces caused by the yaw angle of force line at a large coupler yaw angle are balanced by the locomotive secondary suspension. The lateral forces are transferred to the wheelset by the bogie, which

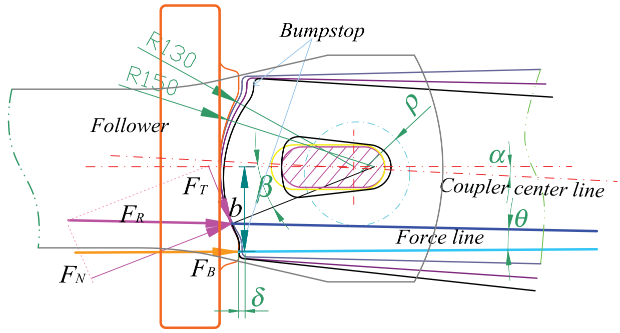

Figure 6. The contact analysis of the end arc surfaces with bumpstop.

will cause the increasing of wheelset lateral forces. Once the coupler lateral forces cannot be balanced, the locomotive derailment will happen. Thus increasing the secondary lateral stiffness of locomotives can be an effective way to improve the stability of the coupler.

3.2. Adding a restoring bumpstop at the end of the coupler

Referring to the geometric and force analysis in Section 2, the significant advantage for this type of coupler is that the coupler lateral forces are small, which is conducive to reducing the side wear of rim. However, the potential coupler instability can cause serious accidents because there is no mechanism to limit the increased yaw angle. An effective method is proposed to improve the stability of the coupler by adding a restoring bumpstop at the end of the coupler, as shown in Figure 6.

3.3. Increasing the arc radii at the end of the coupler

According to the coupler geometric analysis, the arc radii determine the lateral positions of the contact points even at the same coupler yaw angle. Increasing the arc radii at the end of the coupler with a certain range is conducive to increasing the lateral position Y_c and the contact angle β. Two optimisation schemes are proposed and the comparison with the original scheme is conducted. For the first scheme, the follower radius R is 180 mm and the coupler end radius r is 160 mm. For the second scheme, the follower radius R is 200 mm and the coupler end radius r is 180 mm.

3.4. Changing the clearance and stiffness of secondary lateral stopping block

It can be concluded that this type of coupler exhibits self-stabilisation and a smaller lateral force at a small yaw angle when it is compressed. At a larger angle, the coupler lateral forces are balanced by the secondary suspension of the locomotive. Changing the clearance and the stiffness of secondary lateral stopping block can also be taken as an effective way to improve the stability of the coupler.

4. Multi-locomotive dynamic simulation model

In order to verify the theoretical analysis and the effects of four schemes on the stability of the coupler, the multi-body dynamics software was used to build the locomotive and the detailed coupler model. The simple train model composed of four locomotives and three detailed coupler models were established to simulate the process of emergency braking and coupler overturn with appropriate boundary conditions. The stability analyses of the coupler were conducted for each scheme.

4.1. The locomotive dynamic model

Based on the locomotive dynamic model introduced in [15,18], we established the locomotive and the detailed coupler model. The model has four locomotives and three couplers, as shown in Figure 7. The emergency braking is simulated by the braking torques applied to each wheelset. Besides, the longitudinal impulse during the emergency braking is simulated by the two longitudinal forces applied to the both ends of the locomotives respectively. The middle locomotive is taken as focus for these studies.

4.2. The coupler dynamic model

The No. 18 contact force element and the No. 100 nonlinear friction force element of SIMPACK were used to simulate the arc surface contact of the coupler. The coupler dynamic model is composed of five rigid bodies, as shown in Figure 8. The follower has the freedom to move longitudinally and pitch, and the coupler has the freedom to move longitudinally, laterally and yaw. The upper and lower envelope curves are setting by No. 105 force element to simulate the buffer characteristics.

4.3. The boundary conditions and calculation conditions

According to the boundary conditions and the calculation conditions introduced in [15,18], we conducted the dynamics simulation. The maximum coupler longitudinal impact force was set at 2500 kN. The initial speed before braking was 80 km/h and the

Figure 7. The simple train model composed of four locomotives and three couplers.

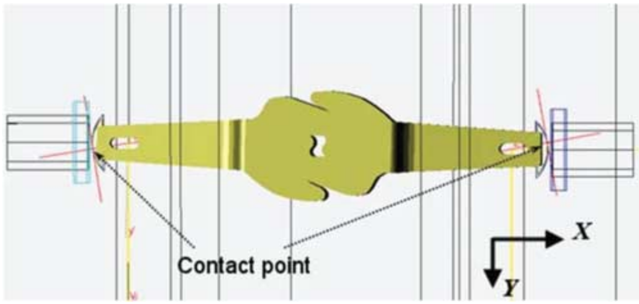

Figure 8. The coupler dynamic model.

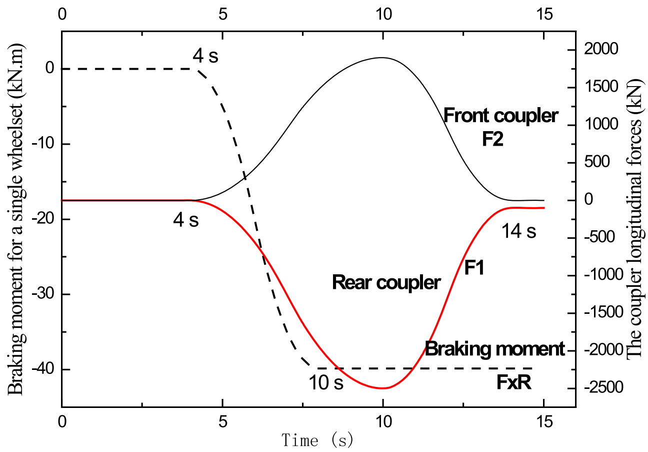

Figure 9. The boundary conditions and calculation conditions.

braking force for a single locomotive was set at 255 kN. The track irregularity of AAR5 is used. The simulation boundary conditions are shown in Figure 9.

5. The simulation results of the coupler stability

5.1. The results for increasing the secondary lateral stiffness of locomotives

According to the simulation results, the coupler yaw instability occurs once the friction coefficient of the arc contact surfaces is smaller than a certain value. This minimum friction coefficient is defined as required minimum friction coefficient.

The results for increasing the secondary lateral stiffness of locomotives are shown in Figure 10. As the maximum coupler longitudinal force increases, a larger required minimum friction coefficient is needed. The required minimum friction coefficient of arc surface decreases as the secondary lateral stiffness of locomotives increases. When the secondary lateral stiffness increases to two times, the required minimum friction coefficient decreases from 0.18 to 0.16 on condition that the maximum coupler longitudinal force is 1000 kN. Likewise the required minimum friction coefficient decreases from 0.26 to 0.22 when the maximum coupler longitudinal force is 1500 kN. And the required minimum friction coefficient decreases from 0.34 to 0.3 when the maximum coupler longitudinal

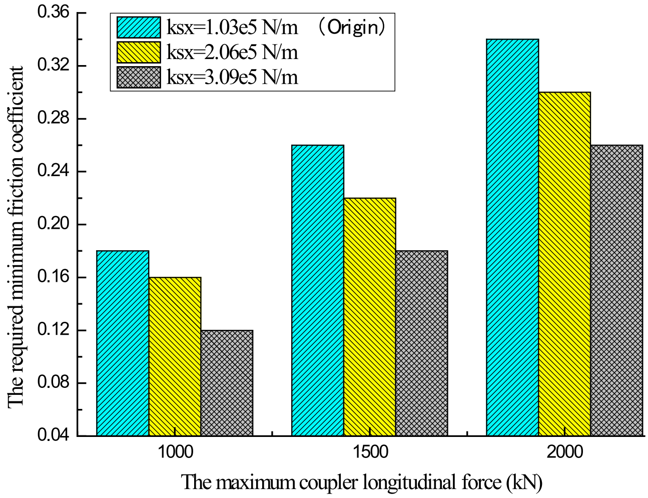

Figure 10. The required minimum friction coefficients with different secondary lateral stiffness.

force is 2000 kN. When the secondary lateral stiffness increases to three times, the effects are more pronounced. The required minimum friction coefficient decreases from 0.18 to 0.12, 0.26 to 18 and 0.34 to 0.26 in case that the maximum coupler longitudinal force is 1000, 1500 and 2000 kN, respectively. It can be concluded that as the secondary lateral stiffness of locomotives increases, the required minimum friction coefficient decreases which is conducive to improve stability of the coupler.

5.2. The results for adding a restoring bumpstop at the end of the coupler

For the case of adding a restoring bumpstop at the end of the coupler, the required minimum friction coefficients for the coupler stability were obtained, as shown in Figure 11. As the bumpstop gap increases, the required minimum friction coefficient increases. The required minimum friction coefficient is 0.34 on condition that the maximum coupler longitudinal force is 2000 kN. While the coupler will be stable when the arc friction coefficient is 0.1 and the bumpstop gap is 5 mm. The wheelset lateral forces with different bumpstop gaps are shown in Figure 12. The maximum coupler longitudinal force is 1500 kN and the bumpstop gaps are 5, 7 and 9 mm, respectively. It can be seen that the wheelset lateral forces decrease significantly as the bumpstop gap decreases and 5 mm bumpstop is the best. Figures 13 and 14 show the coupler yaw angles in simulation process before and after adding bumpstop at the end of the coupler respectively, and the bumpstop gap is 5 mm. The maximum coupler yaw angles before and after adding the bumpstop are about 12° and 4°. The coupler yaw angles are limited within a smaller range by adding a bumpstop at the end of the coupler when the coupler becomes unstable. It is obvious that the stability of the coupler can be improved significantly by adding a bumpstop with the smaller bumpstop gap at the end of the coupler.

5.3. The results for increasing the arc radii at the end of coupler

For the scheme of changing the arc radii at the end of coupler, the results are shown in Figure 15. The required minimum friction coefficients for three cases are 0.34, 0.16 and

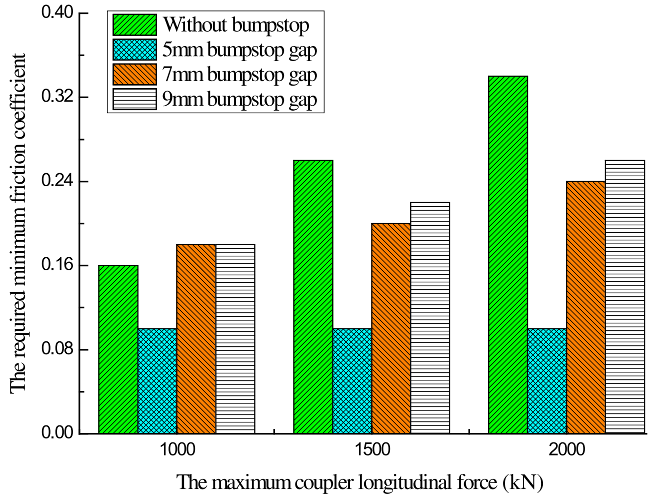

Figure 11. The required minimum friction coefficients with different bumpstop gaps.

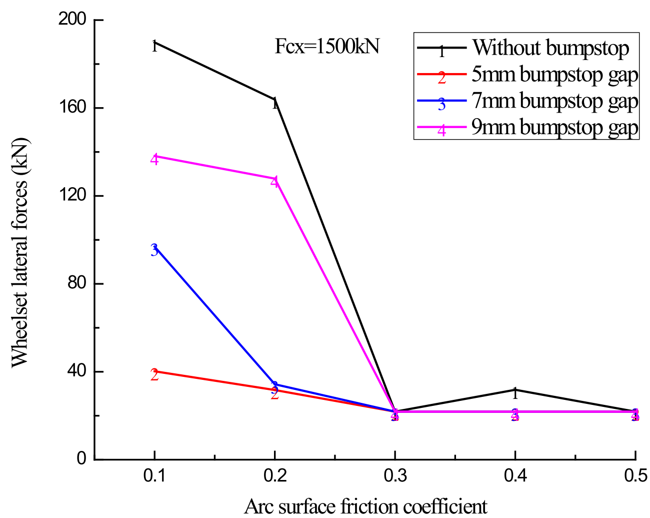

Figure 12. The wheelset lateral forces with different bumpstop gaps.

0.14, respectively on condition that the maximum coupler longitudinal force is 2000 kN. Compared to the original parameters, the corresponding required minimum friction coefficients decrease from 0.34 to 0.16 and 0.14 respectively for the scheme of the R is 180 mm, the r is 160 mm and the scheme of the R is 200 mm, the r is 180 mm when the maximum coupler longitudinal force is 2000 kN. The corresponding required minimum friction coefficients decrease 0.26 to 0.14 and 0.12 respectively on condition that the maximum coupler longitudinal force is 1500 kN. The required minimum friction coefficient decreases as the arc radii increase which indicates that increasing the arc radii at the end of the coupler within a certain range is conducive to improving the stability of the coupler.

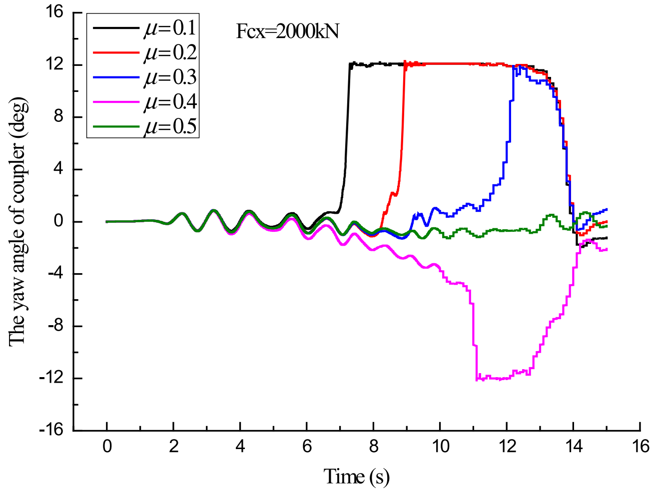

Figure 13. The coupler yaw angle before adding bumpstop.

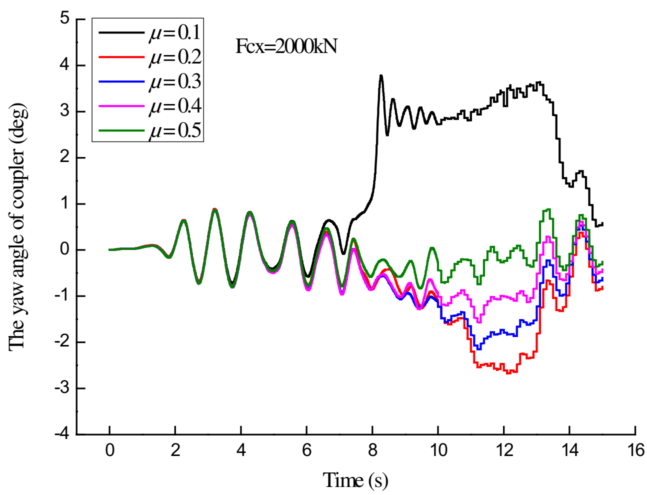

Figure 14. The coupler yaw angle after adding bumpstop.

5.4. The results for changing the clearance and stiffness of secondary lateral stopping block

For the scheme of changing the clearance and stiffness of secondary lateral stopping block, the results are shown in Figure 16. The maximum coupler longitudinal force is 1500 kN and the original stiffness of secondary lateral stopping block is 1.11 kN/mm. The required minimum friction coefficient decreases as the stiffness of secondary lateral stopping block increases and the clearance of secondary lateral stopping block decreases. The required minimum friction coefficient decreases from 0.26 to 0.22 when the stiffness of secondary lateral stopping block increases to eight times. The effects of decreasing the clearance of secondary lateral stopping block are more remarkable. The required minimum friction

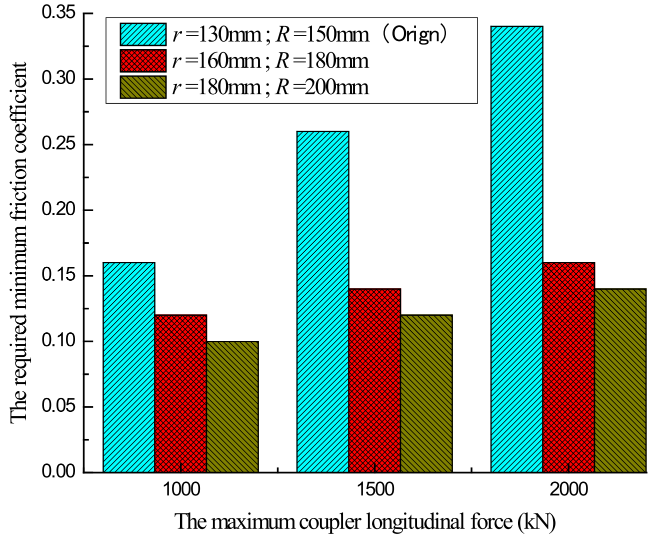

Figure 15. The required minimum friction coefficient for three cases.

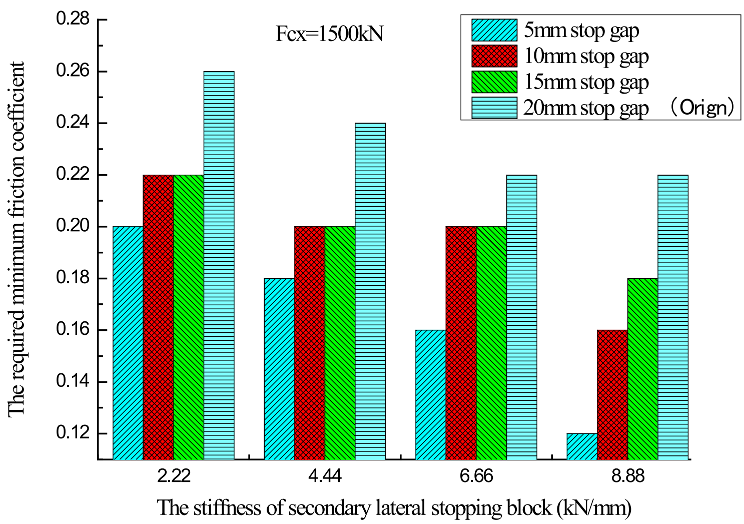

Figure 16. The required minimum friction coefficients with different stiffness and stop gaps of secondary lateral stopping block.

coefficient decreases from to 0.26 to 0.2 when the clearance of secondary lateral stopping block decreases from 20 to 5 mm and the stiffness of secondary lateral stopping block increases to two times. Compared to the original parameters, the required minimum friction coefficient decreases from 0.26 to 0.12 in case that the stiffness of secondary lateral stopping block increases to eight times and the clearance decreases to 5 mm. It can be concluded that increasing the stiffness of secondary lateral stopping block as well as reducing the stop gap is conducive to improving the stability of the coupler.

6. Conclusions

(1) The proposed four improvements based on the structural characteristics and stability mechanism can effectively improve the stability of the coupler with arc surface contact.

(2) For the scheme of increasing the secondary lateral stiffness of locomotives, the results show that the larger required minimum friction coefficient is needed for the larger maximum coupler longitudinal force. When the secondary lateral stiffness increases to three times, the minimum friction coefficient decreases from 0.18 to 0.12 on condition that the maximum coupler longitudinal force is 1000 kN, and the minimum friction coefficient decreases from 0.26 to 0.18 when the maximum coupler longitudinal force is 1500 kN and the minimum friction coefficient decreases from 0.34 to 0.26 when the maximum coupler longitudinal force is 2000 kN. As the secondary lateral stiffness of locomotives increases, the required minimum friction coefficient decreases which is conducive to improve stability of the coupler.

(3) For the scheme of adding a restoring bumpstop at the end of the coupler, the results show that the stability of the coupler can be improved significantly by adding a bumpstop at the end of coupler. The coupler yaw angle can be limited within a small range. As the bumpstop gap increases, the required minimum friction coefficient increases.

(4) For the schemes of changing the arc radii at the end of coupler, the results show that the required minimum friction coefficient decreases as the arc radii increase within a certain range. Compared to the original scheme, the corresponding required minimum friction coefficients decrease from 0.34 to 0.16 and 0.14 for the scheme of the R is 180 mm, the r is 160 mm and the scheme of the R is 200 mm, the r is 180 mm when the maximum coupler longitudinal force is 2000 kN.

(5) For the scheme of changing the clearance and stiffness of secondary lateral stopping block, the results show that the required minimum friction coefficient decreases as the stiffness of secondary lateral stopping block increases and the clearance of secondary lateral stopping block decreases. It decreases from 0.26 to 0.12 in case that the stiffness of secondary lateral stopping block increases to eight times and the clearance decreases to 5 mm.

Disclosure statement

No potential conflict of interest was reported by the authors.

Funding

The material in this paper is based on work supported by grants (51675443, 51735012, 51405404) from the National Natural Science Foundation of China, Key Laboratory grant (2015TPL_T10, 2017TPL_T02) of the Independent Research and Development Projects, and Research Innovation Team grant (17TD0040) of Sichuan Provincial University.

References

[1] Pugi L, Rindi A, Ercole AG, et al. Preliminary studies concerning the application of different braking arrangements on Italian freight trains. Veh Syst Dyn. 2011;49:1339–1365.

[2] Ma W, Luo S, Song R. Coupler dynamic performance analysis of heavy haul locomotive. Veh Syst Dyn. 2012;50:1435–1452.

[3] Mousavi zadeh Noughabi SM, Dehghani K, Pouranvari M. Failure analysis of automatic coupler SA-3 in railway carriages. Eng Fail Anal. 2007;14:903–912.
[4] Transportation Safety Board of Canada (Railway investigation report R02C0050). Ottawa: Transportation Safety Board of Canada; 2002. Derailment, Canadian National Train Number A-442-51-08 Mile 52.1.
[5] Belforte P, Cheli F, Diana G, et al. Numerical and experimental approach for the evaluation of severe longitudinal dynamics of heavy freight trains. Veh Syst Dyn. 2008;46:937–955.
[6] Cole C, Mitchell M, Dudley R, et al. Heavy haul coal train dynamics simulation comparisons of the COALlink and central Queensland systems. Proceedings of the 7th international heavy haul conference; 2001 June 10–14. Brisbane, Australia. p. 217–223.
[7] Simson SA, Cole C. Simulation of curving at low speed under high traction for passive steering hauling locomotives. Veh Syst Dyn. 2008;46:1107–1121.
[8] Cole C, Sun YQ. Simulated comparisons of wagon coupler systems in heavy haul trains. Proc IMechE, Part F: J Rail Rapid Transit. 2006;220:247–256.
[9] Durali M, Shadmehri B. Nonlinear analysis of train derailment in severe braking. J Dyn Syst Meas Control, ASME. 2003;125:48–53.
[10] Design Features for AAR-Approved Special Coupler bodies. AAR Manual of Standards and Recommended Practises Section S, M-211 Appendix E, Page 183, Association of American Railroads. USA, 2010.
[11] Xu ZQ, Ma WH, Wu Q, et al. Coupler rotation behavior and its effect on heavy haul trains. Veh Syst Dyn. 2013;51:1818–1838.
[12] Shi ZY, Wang KY, Guo LR, et al. Effect of arc surfaces friction coefficient on coupler stability in heavy haul locomotives: simulation and experiment. Veh Syst Dyn. 2017: 1–16.
[13] Yao Y, Zhang X-X, Zhang H-J, et al. The stability mechanism and its application of heavy haul couplers with arc surface contact. Veh Syst Dyn. 2013;51:1324–1341.
[14] Wu Q, Luo S, Xu Z, et al. Coupler jackknifing and derailments of locomotives on tangent track. Veh Syst Dyn. 2013;51:1784–1800.
[15] Yao Y, Liu X, Zhang H, et al. The stability and mechanical characteristics of heavy haul couplers with restoring bumpstop. Veh Syst Dyn. 2014;52:26–44.
[16] Ma WH, Luo SH, Song RR. Coupler dynamic performance analysis of heavy haul locomotives. Veh Syst Dyn. 2012;50:1–18.
[17] Qu T, Ma W, Wu D, et al. Influence of coupler and buffer on dynamics performance of heavy haul locomotive. Open Mech Eng J. 2015;9:1033–1038.
[18] Yao Y, Zhang X, Zhang H. Dynamic performances of an innovative coupler used in heavy haul trains. Veh Syst Dyn. 2014;52:1288–1303.